
UPPER BOUNDS ON OVERSHOOT IN SIR MODELS WITH NONLINEAR INCIDENCE

Maximilian M. Nguyen

Lewis-Sigler Institute
Princeton University
Princeton, NJ 08544

mmnguyen@princeton.edu

April 5, 2024

ABSTRACT

We expand the calculation of the upper bound on epidemic overshoot in SIR models to account for nonlinear incidence. We lay out the general procedure and restrictions to perform the calculation analytically. We demonstrate the procedure by working through several examples and also numerically study what happens to the upper bound on overshoot when nonlinear incidence manifests in the form of epidemic dynamics over a contact network. We find that both steeper incidence terms and larger contact heterogeneity can increase the range of communicable diseases at which the overshoot remains a relatively large public health hazard.

Introduction

Compartmental models have been an invaluable tool for analyzing the dynamics of epidemics for the last century. In particular, the susceptible-infected-recovered (SIR) model has long been a workhorse compartmental model for describing transient epidemics due to its relative simplicity and has received a lot of attention in both the academic literature and the public health arena [1, 2]. The mechanism of transmission of a communicable disease underlying this model and a variety of other contagion models is contact between healthy and infectious individuals, which results in conversion of the healthy individuals into an infected state. Choosing how to precisely define the transmission interaction between healthy and infectious individuals leads to a variety of models depending on the assumptions made. For instance, in a spatially-explicit model, one might represent the contact between individual members of the population by means of a network. Alternatively, if one is willing to assume all individuals within a compartment are identical, one can formulate a model using ordinary differential equations (ODEs) by assuming an incidence term for how the susceptible and infected compartments mix and generate new infected individuals.

The quintessential SIR ODE model, known as the Kermack-McKendrick model, is shown in (1-3). The model assumes a bilinear incidence rate βSI for the growth term of the infected compartment, with transmissibility parameter β and first-order (i.e. linear) with respect to the fraction of population that is susceptible (S) and infected (I).

$$\frac{dS}{dt} = -\beta SI \tag{1}$$

$$\frac{dI}{dt} = \beta SI - \gamma I \tag{2}$$

$$\frac{dR}{dt} = \gamma I \tag{3}$$

While a bilinear incidence rate between healthy and infected individuals can be a reasonable first assumption, depending on the real-world situation being modeled and the level of precision required, the assumption can be insufficient or inaccurate. A significant body of work in the literature has been done to generalize this incidence term into more

detailed forms [3–8]. Moving beyond bilinear forms towards nonlinear incidence allows for the consideration of models with more biological complexity and realism. Factors such as network effects, seasonality, and non-pharmaceutical interventions are known to give rise to more complex dynamics [9–12]. The studying of nonlinear transmission in the context of epidemiology here is a specific case of a larger growing interest across a range of fields in studying the effects of transmission dynamics in complex systems. The exploration of interactions beyond the bilinear form has taken place in contexts ranging from social dynamics [13–17], ecology [18–21], economics [22, 23], to molecular biology [24]. Significant effort has also been expended on synthesizing these ideas into a more general model of contagion that can be used in different domains [25–27].

As the representation of transmission is arguably the most important aspect in setting up a model of communicable disease, the choice for the incidence rate has downstream consequences on many epidemiological quantities of interest. These include, but are not limited too, the epidemic size, the herd immunity threshold, epidemic duration, and the epidemic overshoot. While features such as the epidemic size and the herd immunity threshold have been studied rather extensively in the literature, the behavior of overshoot remains relatively under explored, in particular for more general incidence rates.

Overshoot is a concept from mathematics and control theory that quantifies the amount of excess from when a function exceeds its target value [28, 29]. This concept has been applied to a variety of contexts ranging from ecological and environmental problems that pertain to overconsumption and sustainability [30–33] to biotechnology that controls blood flow [34]. In the epidemiological context, the overshoot quantifies the number of individuals that become infected after the prevalence peak of infections occurs. In simple epidemics, as the peak of the epidemic coincides with the threshold at which transmission is sufficiently reduced so that the epidemic is no longer growing, the overshoot reflects the excess in cases beyond this minimal threshold of protection.

While the terminology *excess* may give the connotation of a relatively small effect, in the the Kermack-McKendrick SIR model it can be shown that up to nearly 30% of the population can become infected in the overshoot phase of the epidemic [35]. This is also not a rare case, as large values of overshoot occur at rather common values for the basic reproduction (R_0) of 1.5 – 4, which includes communicable diseases such as COVID-19 [36–38], HIV [39], and influenza [40]. An analysis of data from the the first wave of the COVID-19 pandemic in the urban city of Manaus, Brazil [35, 41], where disease spread went largely unmitigated, suggested that the dynamics could be reasonably approximated by the Kermack-McKendrick SIR model and that nearly 30% of the population became infected in the overshoot phase.

The overshoot highlights the potentially large public-health risk that can be posed by allowing for unmitigated spread or reducing intervention measures prematurely. However, the transmission rates at which the overshoot poses the greatest risk depends on the form of the incidence rate, which drives the need to understand the behavior for incidence beyond the simple bilinear case. As the overshoot quantifies the excess number of cases that occur after the herd immunity threshold has been reached, it is also intimately connected with any potential interventions or mitigation strategies. A question of great concern to epidemiologists and public health officials is figuring out the optimal control strategies for reducing excess cases and mortality [42–45]. Any optimal strategy by design generally seeks to eliminate the overshoot. Thus, a better understanding the behavior of overshoot under different model assumptions might allow for better control measures to be designed and developed.

While the overshoot within the SIR model has received some attention [42, 46–48], a detailed understanding of its full mathematical behavior within compartmental models remains incomplete. An observation that the overshoot is largest for intermediate basic reproduction numbers was first numerically observed by Zarnitsyna et al. [49]. An explanation for that phenomena in the context of the Kermack-McKendrick model was recently discovered, showing that the overshoot is derived from a trade-off from the basic reproduction number in driving both the final epidemic size and how quickly the disease burns through the population [35]. Here we lay the foundation to calculate the upper bound for overshoot when considering incidence terms beyond the simple bilinear case. We will first derive the behavior of the overshoot for more general incidence rates within the context of ODE models, where the results and understanding can be analytical and precise. As nonlinear incidence can also arise through the connectivity structure of networks, we will then numerical explore the effect of network structure and changing network topologies on overshoot.

Results

Effect of Nonlinear Incidence on Overshoot in SIR ODE Models

We first examine the effect of nonlinear incidence on overshoot for ODE models, where the computations can be made analytical. The equations of the Kermack-McKendrick SIR ODE model are given as follows with generic incidence term $\beta f(S)g(I)$, where $f(S)$ and $g(I)$ are functions of S and I respectively to be specified.

$$\frac{dS}{dt} = -\beta f(S)g(I) \quad (4)$$

$$\frac{dI}{dt} = \beta f(S)g(I) - \gamma I \quad (5)$$

$$\frac{dR}{dt} = \gamma I \quad (6)$$

where $S, I, R \in [0, 1]$ are the fractions of the population that are susceptible, infected, and recovered respectively, $\beta, \gamma \in \mathbb{R}_{>0}$ are positive-definite parameters for transmission and recovery rate respectively.

For the SIR model, the overshoot is given by the following equation:

$$\text{Overshoot} = S_{t^*} - S_\infty \quad (7)$$

where S_{t^*} is the fraction of susceptibles at the time of the prevalence peak (i.e. when I is maximal in value), t^* , and S_∞ is the fraction of susceptibles at the end of the epidemic. To solve this equation, the easiest approach is to derive an equation for S_{t^*} in terms of only S_∞ and parameters. We do this by first setting (5) equal to 0 and solving for the critical susceptible fraction S_{t^*} .

$$\frac{dI}{dt} = 0 = \beta f(S_{t^*})g(I_{t^*}) - \gamma I_{t^*} \quad (8)$$

By using the usual definition for the basic reproduction number, $R_0 \equiv \frac{\beta}{\gamma}$, we obtain the following equation for S_{t^*} .

$$S_{t^*} = f^{-1}\left(\frac{I_{t^*}}{g(I_{t^*})} \frac{1}{R_0}\right)$$

We can see from this equation that S_{t^*} will have I dependence unless $g(I_{t^*}) = I_{t^*}$. Thus to make what follows analytically tractable, let us assume $g(I_{t^*}) = I_{t^*}$. We will provide even stronger justification why $g(I)$ must take this form later in the results. This assumption of $g(I_{t^*}) = I_{t^*}$ reduces the above equation to the following.

$$S_{t^*} = f^{-1}\left(\frac{1}{R_0}\right) \quad (9)$$

Taking this equation for S_{t^*} (9) and the overshoot formula (7), we obtain:

$$\text{Overshoot} = f^{-1}\left(\frac{1}{R_0}\right) - S_\infty \quad (10)$$

Thus the main challenge now becomes a problem of finding an equation for R_0 and the inverse function f^{-1} . Based on previous results [35], the following outlines the general steps for calculating the maximal overshoot for a SIR model:

- A. Take the ratio of $\frac{dI}{dt}$ and $\frac{dS}{dt}$. Integrate the resulting ratio. The indefinite integral requires a constant of integration, which is a conserved quantity that applies at every time point along the system's trajectory in time.
- B. Evaluate the equation for the conserved quantity at the beginning of the epidemic ($t = 0$) and the end of the epidemic ($t = \infty$) using initial conditions and asymptotic values. Then, rearrange the resulting equation for $\frac{1}{R_0}$.
- C. Find the form for the inverse function, f^{-1} .
- D. Combine the equations for $\frac{1}{R_0}$ and f^{-1} with the overshoot equation.

E. Maximize the resulting overshoot equation by taking the derivative of the equation with respect to S_∞ and setting the equation to 0 to find the extremal point S_∞^* . This step usually leads to a transcendental equation for S_∞^* , which can be solved numerically.

F. Use the maximizing S_∞^* value in the overshoot equation to calculate the corresponding maximal overshoot.

G. Calculate the corresponding R_0^* using S_∞^* and the $\frac{1}{R_0}$ equation.

Thus, the analytical exploration of nonlinear incidence terms of the type $\beta f(S)g(I)$ is reduced to exploring different forms of $f(S)$.

Restrictions on $g(I)$

The first step is to rule out what forms for the incidence term will not work with the procedure outlined above.

We now show the principle reason why we require $g(I) = I$. We can see from calculating Step A. in (11) that any incidence term that does not take the form $g(I) = aI, a \in \mathbb{R}$, where a is a real scalar, retains I dependence upon simplification.

$$\text{Step A.: } \frac{\frac{dI}{dt}}{\frac{dS}{dt}} = \frac{\beta f(S)g(I) - \gamma I}{-\beta f(S)g(I)} = -1 + \frac{I}{R_0 f(S)g(I)} \quad (11)$$

Any deviation from the form $g(I) = aI$ results in I in the numerator and the denominator not completely cancelling out which will result in having to integrate I with respect to S , which we will not be able to do analytically. Therefore, I must enter linearly into the incidence term. Since a can be absorbed into the β parameter, all possible incidence terms for the purpose of calculating overshoot analytically will take the form $\beta \cdot f(S) \cdot I$.

Restrictions on $f(S)$

We now turn to what restrictions there are on the form of $f(S)$. We start first with the two boundary conditions for S . First, we must enforce that:

$$f(S = 0) = 0 \quad (12)$$

Otherwise, since I does not have such a restriction, violating this condition leaves open the possibility of having $\frac{dS}{dt}$ (4) be non-zero when the number of susceptibles is zero, which is not realistic.

For the second boundary condition, we must have that:

$$f(S = 1) > \frac{\gamma}{\beta} = \frac{1}{R_0} \quad (13)$$

This is obtained by inspecting $\frac{dI}{dt}$ (5) and ensuring that the incidence term $\beta f(S)g(I)$ is larger than the recovery term γI at $t = 0$ by having a sufficiently high β . Otherwise, the epidemic never starts. Assuming I_0 is sufficiently small, then S is approximately 1 at $t = 0$.

Beyond the boundary conditions, an obvious requirement is that $f(S)$ should be a continuous function. In order to be able to calculate the maximal overshoot analytically, the function should be integrable with respect to S and should also have a closed-form inverse f^{-1} . As we will demonstrate, non-monotonic functions for $f(S)$ are possible.

For $f(S)$, the following examples are constructed using basic functions that satisfy the above criteria:

1. $\exp(S) - 1$
2. Invertible polynomials of S
3. $\sin(aS)$

Conversely, there are many examples of functions that would not work. An example that satisfies the boundary conditions but that does not have a closed form inverse is $f(S) = \log(S + 1)$. While similar to examples listed, the following violate the boundary conditions: $\exp(S)$, $\log(S)$, $\cos(S)$. Examples that violate conditions of continuity include step functions of S or $f(S)$ with cusps.

Deriving Maximal Overshoot for Various $f(S)$

As an example, we will now look at a model with nonlinear incidence and apply the whole procedure previously outlined for finding the maximal overshoot.

Example: $f(S) = \exp(S) - 1$

Let us consider an incidence rate that takes on an exponential form. This produces an incidence term that grows slightly faster than the original bilinear incidence term, and so might be relevant in situations where there are network effects. We start at Step A. by solving for the rate of change of I as a function of S by taking the ratio of $\frac{dI}{dt}$ and $\frac{dS}{dt}$.

$$\frac{dI}{dS} = -1 + \frac{1}{R_0(e^S - 1)} \quad (14)$$

from which it follows on integration using the substitution $u = e^S$ and partial fractions ($\frac{1}{u-1}$ and $\frac{1}{u}$) that $I + S + \frac{S - \ln|e^S - 1|}{R_0}$ is constant along all trajectories.

For Step B., consider the conserved quantity at both the beginning ($t = 0$) and end ($t = \infty$) of the epidemic.

$$I_0 + S_0 + \frac{S_0 - \ln|e^{S_0} - 1|}{R_0} = I_\infty + S_\infty + \frac{S_\infty - \ln|e^{S_\infty} - 1|}{R_0}$$

hence

$$\frac{1}{R_0} = \frac{I_\infty + S_\infty - I_0 - S_0}{S_0 - S_\infty + \ln\left(\frac{|e^{S_\infty} - 1|}{|e^{S_0} - 1|}\right)} \quad (15)$$

We use the initial conditions: $S_0 = 1 - \epsilon$ and $I_0 = \epsilon$, where ϵ is the (infinitesimally small) fraction of initially infected individuals. We use the standard asymptotic of the SIR model that there are no infected individuals at the end of an SIR epidemic: $I_\infty = 0$. This yields:

$$\frac{1}{R_0} = \frac{S_\infty - 1}{1 - S_\infty + \ln\left(\frac{|e^{S_\infty} - 1|}{e - 1}\right)} \quad (16)$$

For Step C., we find the inverse of f .

$$f(x) = e^S - 1 \implies f^{-1}(x) = \ln(x + 1) \quad (17)$$

For Step D., we substitute the expression for $\frac{1}{R_0}$ (16) and f^{-1} (17) into the overshoot equation (10).

$$Overshoot = \ln\left(\frac{\ln\left(\frac{|e^{S_\infty} - 1|}{e - 1}\right)}{1 - S_\infty + \ln\left(\frac{|e^{S_\infty} - 1|}{e - 1}\right)}\right) - S_\infty \quad (18)$$

For Step E., differentiation of both sides with respect to S_∞ and setting the equation to zero to solve for the critical S_∞^* yields:

$$0 = \left(\frac{\ln\left(\frac{|e^{S_\infty^*} - 1|}{e - 1}\right)}{1 - S_\infty^* + \ln\left(\frac{|e^{S_\infty^*} - 1|}{e - 1}\right)}\right)^{-1} \cdot \frac{(1 - S_\infty^* + \ln\left(\frac{|e^{S_\infty^*} - 1|}{e - 1}\right)) \cdot ((\frac{|e^{S_\infty^*} - 1|}{e - 1})^{-1} \frac{e^{S_\infty^*}}{e - 1}) - (\ln\left(\frac{|e^{S_\infty^*} - 1|}{e - 1}\right)) \cdot (-1 + (\frac{|e^{S_\infty^*} - 1|}{e - 1})^{-1} \frac{e^{S_\infty^*}}{e - 1})}{(1 - S_\infty^* + \ln\left(\frac{|e^{S_\infty^*} - 1|}{e - 1}\right))^2} - 1 \quad (19)$$

Since $e^S - 1$ is positive semi-definite over the unit interval for S , dropping the absolute value symbols and simplifying yields:

$$\ln\left(\frac{e^{S_\infty^*} - 1}{e - 1}\right)\left(\ln\left(\frac{e^{S_\infty^*} - 1}{e - 1}\right) - S_\infty^*\right) = (1 - S_\infty^*)\left(\frac{e^{S_\infty^*}}{e^{S_\infty^*} - 1}\right)$$

which admits both a trivial solution ($S_\infty^* = 1$) and the solution $S_\infty^* = 0.1663\dots$.

For Step F, using the non-trivial solution for S_∞^* in the overshoot equation (18) to obtain the value of the maximal overshoot for this model, $Overshoot^*|_{\beta(e^S - 1)I}$ yields:

$$Overshoot^*|_{\beta(e^S - 1)I} = 0.2963\dots \quad (20)$$

Thus, the maximal overshoot for incidence functions of the form $\beta(e^S - 1)I$ is 0.296\dots.

For Step G., we can calculate the corresponding R_0^* using S_∞^* and (16).

$$R_0^*|_{\beta(e^S - 1)I} = 1.7 \quad (21)$$

This result is verified numerically in Figure 1. Compared to the overshoot in the Kermack-McKendrick model [35, 49], we see that the maximal overshoot is also near 30%. However, we see that overshoot has a much broader distribution over the domain of R_0 , suggesting that exponential incidence rates pose a public health hazard for a greater range of communicable diseases over their bilinear counterparts.

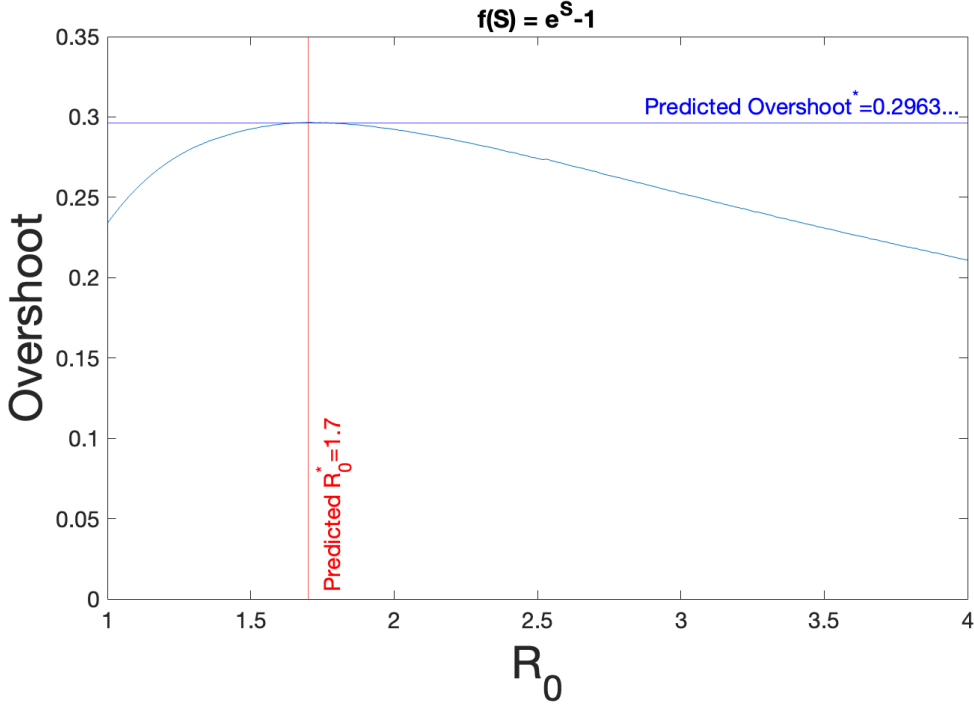


Figure 1: The overshoot as a function of R_0 for an SIR model with nonlinear incidence term of $\beta(e^S - 1)I$. The horizontal line for $Overshoot^*$ in dark blue and the vertical line in red given by $R_0^* = 1.7$ are the theoretical predictions given by the calculations in the text. The curve is obtained from numerical simulations.

Additional examples for incidence rates of a different mathematical form can be found in the Supplemental Information. One example considers when the form of $f(S)$ is given by a polynomial, which can be used to model higher-order effects beyond a simple two-person interaction. Another example considers the consequence of having $f(S)$ that is non-monotonic over the domain of S , which might reflect real scenarios where there are tipping points in behavior.

Nonlinear Incidence Generated from Dynamics on Networks

In the previous sections, we focused on nonlinear incidence that was generated from the introduction of a nonlinearity in an ordinary differential equation model. Importantly, this fundamentally assumes homogeneity in the transmission, in that all infected individuals are identical in their ability to spread the disease further. In contrast, network models allow for heterogeneous spreading which depends on the local connectivity of each infected individual. This provides an entirely different mechanism through which nonlinear incidence can be generated compared to the ordinary differential equation models. As many real-world complexities and details can be more easily captured and explored in a network model, the consequences of those heterogeneities on the overshoot becomes more transparent in network simulations. However, a trade-off for the increased realism is that it becomes more difficult to perform analytical calculations for a general network model, so here we conduct a numerical exploration of the behavior of the overshoot in network models across a range of network structure.

The space of all possible network configurations is immense, so we must restrict ourselves to analyzing a particular subset of possible networks. Here we explore what happens to the overshoot when the contact structure of the population is given by a network graph that is roughly one giant component. While it is possible to construct pathological graphs that produce very complex dynamics, we consider more classical graphs here. Using a parameterization of heterogeneity (σ) given by Ozbay et al. [50] and the configuration model of Newman [51] to randomly construct networks (see Methods for details), we simulated epidemics on a spectrum of networks with structure ranging from the homogeneous limit (well-mixed, complete graph) to a heterogeneous limit (heavy-tailed degree distributions). As the dynamics of the epidemic on a network are stochastic and occur in discrete-time here, they are not parameterized by R_0 as in the ODE models. Instead, we use an analogous parameter that we will denote as a basic reproduction number for networks ($R_{0, \text{network}}$) and is defined as follows:

$$R_{0, \text{network}} \equiv \frac{\tau \cdot \text{Mean Network Degree}}{\rho} \quad (22)$$

The transmission probability (τ) and recovery probability (ρ) are directly analogous to their counterparts (β and γ respectively) in R_0 . The inclusion of the mean network degree as a scalar makes intuitive sense as that represents the average number of potential neighbors an infected node could potentially infect at the beginning of the epidemic, which is analogous to the interpretation of R_0 as the number of secondary infections. We observed what happens to the overshoot on these different graphs as we changed $R_{0, \text{network}}$.

On a network model, where contact structure is made explicit, the homogeneous limit is a complete graph, which recapitulates the well-mixed assumption of the Kermack-McKendrick model. It is not surprising then that the overshoot in the homogeneous graphs ($\sigma \approx 0$) peaks also around 0.3 (Figure 2, *purple* and *blue*), which coincides with the analytical upper bound previously found in the ordinary differential equation Kermack-McKendrick model [35].

We also see that increasing contact heterogeneity (i.e. $\sigma \rightarrow 1$) qualitatively suppresses the overshoot peak both in terms of the overshoot value and the corresponding $R_{0, \text{network}}$. Furthermore, increased heterogeneity also flattens out the overshoot curve as a function of $R_{0, \text{network}}$. We see that for more heterogeneous graphs, the overshoot is larger at very low $R_{0, \text{network}}$. For some intermediate values of contact heterogeneity (Figure 2, *yellow* and *orange*), the overshoot shows larger overshoot than the homogeneous case for large $R_{0, \text{network}}$. This would suggest a larger public health hazard for a larger range of communicable diseases for networks with structure in this regime. The intuition for the larger overshoot at high $R_{0, \text{network}}$ in more heterogeneous networks is that both the peak occurs earlier and that a significant number of cases can occur in the periphery of a network (Figure S3-S5). Since the network core is close to any randomly chosen node in a heterogeneous network, the core becomes more accessible the more heterogeneous the graph is which drives the peak of infections to occur sooner. In the second phase of the epidemic as the epidemic expands out to the periphery the epidemic burns more slowly as individuals in the periphery have fewer neighbors.

However, this trend of a overshoot distribution with a big right tail does not monotonically increase with the contact heterogeneity. We see that at very high amounts of contact heterogeneity, the overall area under this overshoot curve decreases. This can be partially explained by the fact that for very heterogeneous networks, a significant fraction of the population have no neighbors at all. This limits the amount of people that can potentially be infected and caps the outbreak size and subsequently overshoot size.

Discussion

While the overshoot has received less attention and exploration than its epidemiological counterpart (the herd immunity threshold), the overshoot poses a significant potential public health hazard for a large range of communicable diseases when there is no mitigation. Generalizing models to include nonlinear incidence terms allows for the consideration of more real-world effects such as higher-order transmission effects and network effects. Thus, to expand the scope of

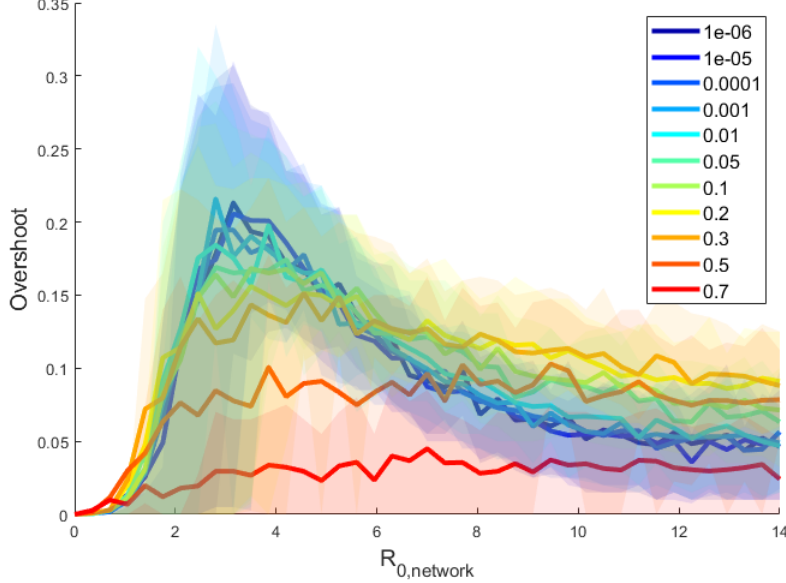


Figure 2: The overshoot for SIR epidemic simulations on networks with varying levels of heterogeneity (σ) as a function of $R_{0, \text{network}}$. Each color shows simulations for networks of different contact heterogeneity as parameterized by σ . The solid lines represent the mean value of 100 simulation runs for a given $R_{0, \text{network}}$ and σ . The shaded areas indicate the 25th and 75th quartiles for those 100 simulations. The other simulation parameters are number of nodes (N) = 200, mean degree of network = 7, and recovery probability (ρ) = 0.2.

previous work, we have illustrated a general method to analytically find the maximal overshoot for generic nonlinear incidence terms.

Starting with the general incidence term $\beta f(S)g(I)$, we have deduced what restrictions must be placed on the form of $f(S)$ and $g(I)$ to make an analytical calculation possible. As long as the conditions for a suitable $f(S)$ are satisfied, in principle the maximal overshoot can be derived. However, in the examples shown in both the main text and supplemental information, we have seen that even relatively simple forms for $f(S)$ can quickly lead to complicated integrals and derivatives. For these examples, we have shown the predictions given by the theoretical calculations generally match the empirical results derived from numerical simulation. From a public-health perspective, we find that incidence rates that are steeper over the domain of S , such as the examples with the exponential or polynomial functions, show a smaller maximal overshoot, but importantly, a much broader range of R_0 's at which the overshoot remains large. As interventions that seek optimal control try to minimize the overshoot, this highlights the need for even stronger interventions when the interactions and subsequent incidence between individuals is higher than a simple bilinear interaction. The example of $f(S) = \sin(aS)$ in the supplemental information is interesting because it can be used to probe the restrictions on the shape of $f(S)$. The case demonstrated that $f(S)$ no longer has to be monotonic over the domain of S , allowing for tipping point-like behavior.

Nonlinear incidence introduced through having a network structure showed that having network connectivity that was more heterogeneous resulted in a reduction in the upper bound on overshoot and a reduction of the dependence of overshoot on transmission overall. Numerically, the overshoot for a homogeneously connected network (i.e. a complete graph) well-approximates a Kermack-McKendrick ODE model. Thus, an upper bound on the overshoot of approximately 0.3 in both models [35] is perhaps unsurprising. While more heterogeneous networks did not have an overshoot larger than 0.3, the overshoot was greater at larger $R_{0, \text{network}}$ than the homogeneous case. Future studies that incorporate more nuanced aspects of behavior, interventions, and time dynamics in the network model can further elucidate the complexities of epidemics on networks.

It will also be interesting to see if more complicated nonlinear interaction terms than the ones presented here can be derived. In addition, it will also be interesting to see how these nonlinear incidence terms interact when additional complexity is added to the SIR model, such as the addition of vaccinations or multiple subpopulations.

Methods

Generating Graphs of Differing Heterogeneity

In Figure 2, we presented the results of SIR simulations of epidemics run on graphs of size $N = 200$ and the mean degree is 7, where the parameter of interest is σ . Each curve represents a different value of the graph heterogeneity. We implemented the following procedure from [50] for generating graphs as a function of a continuous parameter (σ):

The following simple procedure generates a graph that has the desired heterogeneity:

1. Choose values of σ (heterogeneity), the mean node degree (which can be set through the relationship $\text{Mean} = \lambda \Gamma(1 - \frac{1}{\log(\sigma)})$ via σ and an appropriate scale parameter (λ), and N (number of nodes).
2. Draw N random samples from the following distribution using σ and λ , rounding these samples to the nearest integer, since the degree of a node can only take on integer values.

$$f(x; \lambda, \sigma) = \frac{-\ln(\sigma)}{\lambda} \left(\frac{x}{\lambda}\right)^{-\ln(\sigma)-1} e^{-(x/\lambda)^{(-\ln(\sigma))}}; x \geq 0; \sigma \in (0, 1]; \lambda > \mathbb{R}^+$$

3. With the sampled degree distribution from the previous step, now use the configuration model method [51] (which samples over the space of all possible graphs corresponding to a particular degree distribution) to generate a corresponding graph.

This yields a valid graph with the desired amount of heterogeneity as specified by σ .

Simulating Epidemics on Graphs of Differing Heterogeneity

We implemented the following simulation procedure from [50] for implementing an SIR epidemic on a graph:

Given a graph $G(\sigma)$ of heterogeneity σ , fix a transmission probability τ and recovery probability ρ :

1. At time t_0 , fix a small fraction f of nodes to be chosen uniformly on the graph and assign them to the Infected state. The remaining $(1 - f)$ fraction of nodes start as Susceptible.
2. For each $i \in [1, T]$, for each pair of adjacent S and I nodes, the susceptible node becomes infected with probability τ .
3. For each $i \in [1, T]$, each infected node recovers with probability ρ .
4. For each simulation, record the overshoot as the difference between the number of susceptibles at the peak of infection prevalence and the end of the time dynamics.
5. Repeat steps (1-4) n times for each value of τ .
6. Repeat steps (1-5) for each value of σ .

Code for the network simulations is provided in the Supplemental Information.

Numerical Solutions and Code

Where needed, equations were solved numerically using the *ode45* numerical solver in *MATLAB*. Code for the network simulations is provided in the Supplemental Information.

Acknowledgements

The author would like to acknowledge generous funding support provided by the National Science Foundation (DMS-2327711) and a gift from the William H. Miller III.

Author Contributions

M.M.N. designed research, performed research, and wrote and reviewed the manuscript.

Competing Interests

The author declares no competing financial or non-financial interests.

Data Availability Statement

Data sharing is not applicable to this article as no new data were created or analyzed in this study.

References

1. Anderson, R. M. & May, R. M. *Infectious Diseases of Humans: Dynamics and Control* 772 pp. ISBN: 978-0-19-854040-3 (OUP Oxford, Aug. 27, 1992).
2. Diekmann, O., Heesterbeek, H. & Britton, T. *Mathematical Tools for Understanding Infectious Disease Dynamics* 516 pp. ISBN: 978-0-691-15539-5 (Princeton University Press, 2013).
3. Liu, W.-m., Levin, S. A. & Iwasa, Y. Influence of nonlinear incidence rates upon the behavior of SIRS epidemiological models. *Journal of Mathematical Biology* **23**, 187–204. ISSN: 1432-1416. <https://doi.org/10.1007/BF00276956> (2023) (Feb. 1, 1986).
4. Liu, W.-m., Hethcote, H. W. & Levin, S. A. Dynamical behavior of epidemiological models with nonlinear incidence rates. *Journal of Mathematical Biology* **25**, 359–380. ISSN: 1432-1416. <https://doi.org/10.1007/BF00277162> (2023) (Sept. 1, 1987).
5. Hethcote, H. W. & van den Driessche, P. Some epidemiological models with nonlinear incidence. *Journal of Mathematical Biology* **29**, 271–287. ISSN: 1432-1416. <https://doi.org/10.1007/BF00160539> (2023) (Jan. 1, 1991).
6. Ruan, S. & Wang, W. Dynamical behavior of an epidemic model with a nonlinear incidence rate. *Journal of Differential Equations* **188**, 135–163. ISSN: 0022-0396. <https://www.sciencedirect.com/science/article/pii/S002203960200089X> (2023) (Feb. 10, 2003).
7. Jin, Y., Wang, W. & Xiao, S. An SIRS model with a nonlinear incidence rate. *Chaos, Solitons & Fractals* **34**, 1482–1497. ISSN: 0960-0779. <https://www.sciencedirect.com/science/article/pii/S0960077906003882> (2023) (Dec. 1, 2007).
8. Korobeinikov, A. Global Properties of Infectious Disease Models with Nonlinear Incidence. *Bulletin of Mathematical Biology* **69**, 1871–1886. ISSN: 1522-9602. <https://doi.org/10.1007/s11538-007-9196-y> (2023) (Aug. 1, 2007).
9. Pastor-Satorras, R., Castellano, C., Van Mieghem, P. & Vespignani, A. Epidemic processes in complex networks. *Reviews of Modern Physics* **87**. Publisher: American Physical Society, 925–979. <https://link.aps.org/doi/10.1103/RevModPhys.87.925> (2023) (Aug. 31, 2015).
10. Tkachenko, A. V. *et al.* Time-dependent heterogeneity leads to transient suppression of the COVID-19 epidemic, not herd immunity. *Proceedings of the National Academy of Sciences* **118**. Publisher: Proceedings of the National Academy of Sciences, e2015972118. <https://www.pnas.org/doi/abs/10.1073/pnas.2015972118> (2023) (Apr. 27, 2021).
11. Gomes, M. G. M. *et al.* Individual variation in susceptibility or exposure to SARS-CoV-2 lowers the herd immunity threshold. *Journal of Theoretical Biology* **540**, 111063. ISSN: 0022-5193. <https://www.sciencedirect.com/science/article/pii/S0022519322000613> (2023) (May 7, 2022).
12. Montalbán, A., Corder, R. M. & Gomes, M. G. M. Herd immunity under individual variation and reinfection. *Journal of Mathematical Biology* **85**, 2. ISSN: 1432-1416. <https://doi.org/10.1007/s00285-022-01771-x> (2023) (June 30, 2022).
13. Axelrod, R. in *The Complexity of Cooperation* (Princeton University Press, Aug. 18, 1997). ISBN: 978-1-4008-2230-0. <https://www.degruyter.com/document/doi/10.1515/9781400822300/html> (2023).
14. Centola, D. The Spread of Behavior in an Online Social Network Experiment. *Science* **329**. Publisher: American Association for the Advancement of Science, 1194–1197. <https://www.science.org/doi/full/10.1126/science.1185231> (2023) (Sept. 3, 2010).
15. Vespignani, A. Modelling dynamical processes in complex socio-technical systems. *Nature Physics* **8**. Number: 1 Publisher: Nature Publishing Group, 32–39. ISSN: 1745-2481. <https://www.nature.com/articles/nphys2160> (2023) (Jan. 2012).
16. Lehmann, S. & Ahn, Y.-Y. *Complex Spreading Phenomena in Social Systems: Influence and Contagion in Real-World Social Networks* Google-Books-ID: 53hhDwAAQBAJ. 356 pp. ISBN: 978-3-319-77332-2 (Springer, June 21, 2018).
17. Hébert-Dufresne, L., Scarpino, S. V. & Young, J.-G. Macroscopic patterns of interacting contagions are indistinguishable from social reinforcement. *Nature Physics* **16**. Number: 4 Publisher: Nature Publishing Group, 426–431. ISSN: 1745-2481. <https://www.nature.com/articles/s41567-020-0791-2> (2023) (Apr. 2020).

18. Bascompte, J. & Solé, R. V. Rethinking complexity: modelling spatiotemporal dynamics in ecology. *Trends in Ecology & Evolution* **10**. Publisher: Elsevier, 361–366. ISSN: 0169-5347. [https://www.cell.com/trends/ecology-evolution/abstract/S0169-5347\(00\)89134-X](https://www.cell.com/trends/ecology-evolution/abstract/S0169-5347(00)89134-X) (2023) (Sept. 1, 1995).
19. Hofbauer, J. & Sigmund, K. *Evolutionary Games and Population Dynamics* 356 pp. ISBN: 978-0-521-62570-8 (Cambridge University Press, May 28, 1998).
20. Grilli, J., Barabás, G., Michalska-Smith, M. J. & Allesina, S. Higher-order interactions stabilize dynamics in competitive network models. *Nature* **548**. Number: 7666 Publisher: Nature Publishing Group, 210–213. ISSN: 1476-4687. <https://www.nature.com/articles/nature23273> (2023) (Aug. 2017).
21. Taylor, A. & Crizer, A. A Modified Lotka-Volterra Competition Model with a Non-Linear Relationship Between Species. *Rose-Hulman Undergraduate Mathematics Journal* **6**. ISSN: XXXX-XXXX. <https://scholar.rose-hulman.edu/rhumj/vol6/iss2/8> (Jan. 15, 2017).
22. May, R. M., Levin, S. A. & Sugihara, G. Ecology for bankers. *Nature* **451**. Number: 7181 Publisher: Nature Publishing Group, 893–894. ISSN: 1476-4687. <https://www.nature.com/articles/451893a> (2023) (Feb. 2008).
23. Arthur, W. B. Foundations of complexity economics. *Nature Reviews Physics* **3**. Number: 2 Publisher: Nature Publishing Group, 136–145. ISSN: 2522-5820. <https://www.nature.com/articles/s42254-020-00273-3> (2023) (Feb. 2021).
24. Stefan, M. I. & Novère, N. L. Cooperative Binding. *PLOS Computational Biology* **9**. Publisher: Public Library of Science, e1003106. ISSN: 1553-7358. <https://journals.plos.org/ploscompbiol/article?id=10.1371/journal.pcbi.1003106> (2023) (June 27, 2013).
25. Goffman, W. & Newill, V. A. Generalization of Epidemic Theory: An Application to the Transmission of Ideas. *Nature* **204**. Number: 4955 Publisher: Nature Publishing Group, 225–228. ISSN: 1476-4687. <https://www.nature.com/articles/204225a0> (2023) (Oct. 1964).
26. Barrat, A., Barthélémy, M. & Vespignani, A. *Dynamical Processes on Complex Networks* Google-Books-ID: fUAhAwAAQBAJ. 586 pp. ISBN: 978-1-107-37742-4 (Cambridge University Press, Oct. 23, 2008).
27. Centola, D. *How Behavior Spreads: The Science of Complex Contagions* Google-Books-ID: V3GYDwAAQBAJ. 308 pp. ISBN: 978-0-691-17531-7 (Princeton University Press, June 12, 2018).
28. Doyle, J. C., Francis, B. A. & Tannenbaum, A. R. *Feedback Control Theory* Google-Books-ID: zrPDAgAAQBAJ. 264 pp. ISBN: 978-0-486-31833-2 (Courier Corporation, Apr. 9, 2013).
29. Sethi, S. P. in *Optimal Control Theory: Applications to Management Science and Economics* (ed Sethi, S. P.) 1–26 (Springer International Publishing, Cham, 2019). ISBN: 978-3-319-98237-3. https://doi.org/10.1007/978-3-319-98237-3_1 (2023).
30. Catton, W. R. *Overshoot: The Ecological Basis of Revolutionary Change* 324 pp. ISBN: 978-0-252-00988-4 (University of Illinois Press, June 1982).
31. Wackernagel, M. *et al.* Tracking the ecological overshoot of the human economy. *Proceedings of the National Academy of Sciences* **99**. Publisher: Proceedings of the National Academy of Sciences, 9266–9271. <https://www.pnas.org/doi/abs/10.1073/pnas.142033699> (2023) (July 9, 2002).
32. Bradshaw, C. J. A. *et al.* Underestimating the Challenges of Avoiding a Ghastly Future. *Frontiers in Conservation Science* **1**. ISSN: 2673-611X. <https://www.frontiersin.org/articles/10.3389/fcosc.2020.615419> (2023) (2021).
33. Fanning, A. L., O'Neill, D. W., Hickel, J. & Roux, N. The social shortfall and ecological overshoot of nations. *Nature Sustainability* **5**. Number: 1 Publisher: Nature Publishing Group, 26–36. ISSN: 2398-9629. <https://www.nature.com/articles/s41893-021-00799-z> (2023) (Jan. 2022).
34. Rosengarten, B., Osthaus, S. & Kaps, M. Overshoot and Undershoot: Control System Analysis of Haemodynamics in a Functional Transcranial Doppler Test. *Cerebrovascular Diseases* **14**, 148–152. ISSN: 1015-9770. <https://doi.org/10.1159/000065672> (2023) (Oct. 25, 2002).
35. Nguyen, M. M., Freedman, A. S., Ozbay, S. A. & Levin, S. A. Fundamental bound on epidemic overshoot in the SIR model. *Journal of The Royal Society Interface* **20**. Publisher: Royal Society, 20230322. <https://royalsocietypublishing.org/doi/full/10.1098/rsif.2023.0322> (2024) (Dec. 6, 2023).
36. Li, Q. *et al.* Early Transmission Dynamics in Wuhan, China, of Novel Coronavirus-Infected Pneumonia. *New England Journal of Medicine* **382**. Publisher: Massachusetts Medical Society _eprint: <https://doi.org/10.1056/NEJMoa2001316>, 1199–1207. ISSN: 0028-4793. <https://doi.org/10.1056/NEJMoa2001316> (2024) (Mar. 26, 2020).
37. D'Arienzo, M. & Coniglio, A. Assessment of the SARS-CoV-2 basic reproduction number, R_0 , based on the early phase of COVID-19 outbreak in Italy. *Biosafety and Health* **2**, 57–59. ISSN: 2590-0536. <https://www.sciencedirect.com/science/article/pii/S2590053620300410> (2024) (June 1, 2020).

38. Majumder, M. S. & Mandl, K. D. Early transmissibility assessment of a novel coronavirus in Wuhan, China. *Social Science Research Network*, 3524675. ISSN: 1556-5068. <https://www.ncbi.nlm.nih.gov/pmc/articles/PMC7366781/> (2024) (Jan. 24, 2020).
39. Hollingsworth, T. D., Anderson, R. M. & Fraser, C. HIV-1 Transmission, by Stage of Infection. *The Journal of Infectious Diseases* **198**, 687–693. ISSN: 0022-1899. <https://doi.org/10.1086/590501> (2024) (Sept. 1, 2008).
40. Biggerstaff, M., Cauchemez, S., Reed, C., Gambhir, M. & Finelli, L. Estimates of the reproduction number for seasonal, pandemic, and zoonotic influenza: a systematic review of the literature. *BMC Infectious Diseases* **14**, 480. ISSN: 1471-2334. <https://doi.org/10.1186/1471-2334-14-480> (2024) (Sept. 4, 2014).
41. Buss, L. F. *et al.* Three-quarters attack rate of SARS-CoV-2 in the Brazilian Amazon during a largely unmitigated epidemic. *Science* **371**. Publisher: American Association for the Advancement of Science, 288–292. <https://www.science.org/doi/full/10.1126/science.abe9728> (2024) (Jan. 15, 2021).
42. Handel, A., Longini, I. M. & Antia, R. What is the best control strategy for multiple infectious disease outbreaks? *Proceedings of the Royal Society B: Biological Sciences* **274**. Publisher: Royal Society, 833–837. <https://royalsocietypublishing.org/doi/full/10.1098/rspb.2006.0015> (2023) (Dec. 19, 2006).
43. Lauro, F. D., Kiss, I. Z. & Miller, J. C. Optimal timing of one-shot interventions for epidemic control. *PLOS Computational Biology* **17**. Publisher: Public Library of Science, e1008763. ISSN: 1553-7358. <https://journals.plos.org/ploscompbiol/article?id=10.1371/journal.pcbi.1008763> (2023) (Mar. 18, 2021).
44. Morris, D. H., Rossine, F. W., Plotkin, J. B. & Levin, S. A. Optimal, near-optimal, and robust epidemic control. *Communications Physics* **4**. Publisher: Nature Publishing Group, 1–8. ISSN: 2399-3650. <https://www.nature.com/articles/s42005-021-00570-y> (2024) (Apr. 20, 2021).
45. Kollepara, P. K., Chisholm, R. H., Kiss, I. Z. & Miller, J. C. Ethical dilemma arises from optimizing interventions for epidemics in heterogeneous populations. *Journal of The Royal Society Interface* **21**. Publisher: Royal Society, 20230612. <https://royalsocietypublishing.org/doi/full/10.1098/rsif.2023.0612> (2024) (Feb. 7, 2024).
46. Ellison, G. *Implications of Heterogeneous SIR Models for Analyses of COVID-19* June 2020. <https://www.nber.org/papers/w27373> (2023).
47. Rachel, L. An Analytical Model of Covid-19 Lockdowns. *Center for Macroeconomics* (2020).
48. Ketcheson, D. I. Optimal control of an SIR epidemic through finite-time non-pharmaceutical intervention. *Journal of Mathematical Biology* **83**, 7. ISSN: 1432-1416. <https://doi.org/10.1007/s00285-021-01628-9> (2023) (June 26, 2021).
49. Zarnitsyna, V. I. *et al.* Intermediate levels of vaccination coverage may minimize seasonal influenza outbreaks. *PLOS ONE* **13**. Publisher: Public Library of Science, e0199674. ISSN: 1932-6203. <https://journals.plos.org/plosone/article?id=10.1371/journal.pone.0199674> (2022) (June 26, 2018).
50. Ozbay, S. A. & Nguyen, M. M. Parameterizing network graph heterogeneity using a modified Weibull distribution. *Applied Network Science* **8**. Number: 1 Publisher: SpringerOpen, 1–12. ISSN: 2364-8228. <https://appliednetsci.springeropen.com/articles/10.1007/s41109-023-00544-9> (2023) (Dec. 2023).
51. Newman, M. *Networks* Google-Books-ID: YdZjDwAAQBAJ. 793 pp. ISBN: 978-0-19-252749-3 (Oxford University Press, July 4, 2018).

Supplemental Materials: Upper Bounds on Overshoot in SIR Models with Nonlinear Incidence (entire supplement moved from main body of text)

Example 2: $f(S) = \text{Invertible Polynomials of } S$

Next, let us consider invertible polynomials. Having access to large degree polynomials will allow us to make arbitrarily sharp incidence terms. While the set of invertible polynomials is a relatively small subset of all polynomials, it still contains an infinitely large number of possible functions. Because the procedure will require integration of $f(S)$ while it is in the denominator, the algebraic details of doing this for higher-order polynomials with lower-order terms can quickly become cumbersome. So let us illustrate a test case using just the leading term of a generic cubic function. Let $f(S) = aS^3$, where $a \in \mathbb{R}$.

We start at Step A. by solving for the rate of change of I as a function of S by taking the ratio of $\frac{dI}{dt}$ and $\frac{dS}{dt}$.

$$\frac{dI}{dS} = -1 + \frac{1}{R_0 a S^3} \quad (23)$$

from which it follows on integration that $I + S + \frac{1}{2R_0 a S^2}$ is constant along any trajectory.

For Step B., consider the conserved quantity at both the beginning ($t = 0$) and end ($t = \infty$) of the epidemic.

$$I_0 + S_0 + \frac{1}{2R_0 a S_0^2} = I_\infty + S_\infty + \frac{1}{2R_0 a S_\infty^2}$$

hence

$$\frac{1}{R_0} = (I_\infty + S_\infty - I_0 - S_0) \frac{2a(S_0 S_\infty)^2}{S_\infty^2 - S_0^2} \quad (24)$$

Using the initial conditions ($S_0 = 1 - \epsilon$ and $I_0 = \epsilon$, where $\epsilon \ll 1$) and asymptotic condition ($I_\infty = 0$) yields:

$$\frac{1}{R_0} = \frac{2a S_\infty^2}{S_\infty + 1} \quad (25)$$

For Step C., we find the inverse of f .

$$f(x) = ax^3 \implies f^{-1}(x) = \left(\frac{x}{a}\right)^{1/3} \quad (26)$$

For Step D., we substitute the expression for $\frac{1}{R_0}$ (25) and f^{-1} (26) into the overshoot equation (10).

$$\text{Overshoot} = \left(\frac{2S_\infty^2}{S_\infty + 1}\right)^{1/3} - S_\infty \quad (27)$$

For Step E., differentiation with respect to S_∞ and setting the equation to zero to solve for the critical S_∞^* yields:

$$0 = \frac{1}{3} \left(\frac{2S_\infty^{*2}}{S_\infty^* + 1}\right)^{-2/3} \left(\frac{(S_\infty^* + 1) \cdot 4S_\infty^* - 2S_\infty^{*2} \cdot 1}{(S_\infty^* + 1)^2}\right) - 1 \quad (28)$$

whose solution is $S_\infty^* = 0.310\dots$

For Step F., using S_∞^* in the overshoot equation (27) to obtain the value of the maximal overshoot for this model, $\text{Overshoot}^*|_{\beta(aS^3)I}$ yields:

$$\text{Overshoot}^*|_{\beta(aS^3)I} = 0.217\dots \quad (29)$$

Thus, the maximal overshoot for incidence functions of the form $\beta(aS^3)I$ is $0.217\dots$

For Step G., we can calculate the corresponding R_0^* using S_∞^* and (25).

$$R_0^*|_{\beta(aS^3)I} = \frac{6.816\dots}{a} \quad (30)$$

This prediction of the maximal overshoot being independent of a , whereas the corresponding critical R_0 is inversely proportional to a is verified numerical in Figure S1. Furthermore, it can be shown that the independence of the maximal overshoot of a carries holds for any $f(S) = aS^n$. Since a can be absorbed into β , the maximal overshoot is consequently independent of R_0 and instead only depends on the power of S .

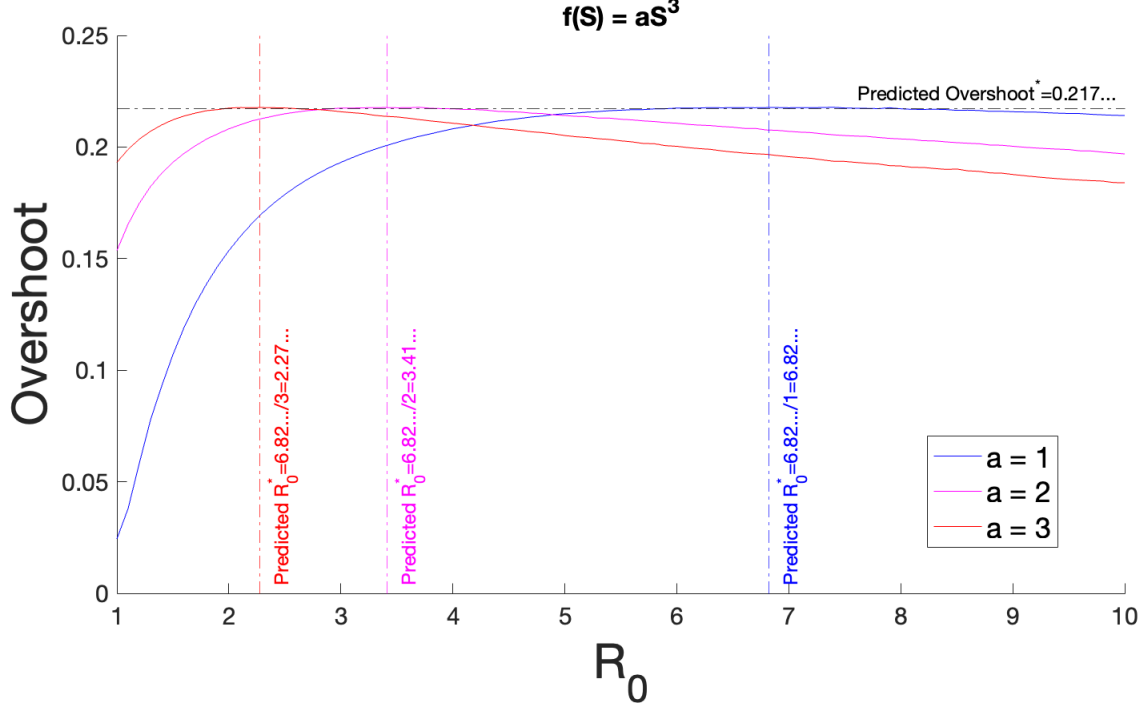


Figure S1: The overshoot as a function of R_0 for an SIR model with nonlinear incidence term of $\beta(aS^3)I$ for different values of a . The dashed horizontal line for $Overshoot^*$ and the dashed vertical lines given by $R_0^* = 1/a$ are the theoretical predictions given by the calculations in the text. The solid curves are obtained from numerical simulations using the value of the a parameter.

Example 3: $f(S) = \sin(aS), a > 0$

We start at Step A. by solving for the rate of change of I as a function of S by taking the ratio of $\frac{dI}{dt}$ and $\frac{dS}{dt}$.

$$\frac{dI}{dS} = -1 + \frac{1}{R_0 \sin(aS)}$$

from which it follows on integration using the substitution $u = \csc(aS) + \cot(aS)$ that $I + S + \frac{\ln|\csc(aS) + \cot(aS)|}{R_0 a}$ is constant along all trajectories.

For Step B., consider the conserved quantity at both the beginning ($t = 0$) and end ($t = \infty$) of the epidemic.

$$I_0 + S_0 + \frac{\ln|\csc(aS_0) + \cot(aS_0)|}{R_0 a} = I_\infty + S_\infty + \frac{\ln|\csc(aS_\infty) + \cot(aS_\infty)|}{R_0 a}$$

hence

$$\frac{1}{R_0} = (I_\infty + S_\infty - I_0 - S_0) \frac{a}{\ln \frac{|\csc(aS_0) + \cot(aS_0)|}{|\csc(aS_\infty) + \cot(aS_\infty)|}} \quad (31)$$

Using the initial conditions ($S_0 = 1 - \epsilon$ and $I_0 = \epsilon$, where $\epsilon \ll 1$) and asymptotic condition ($I_\infty = 0$) yields:

$$\frac{1}{R_0} = \frac{a(S_\infty - 1)}{\ln \frac{|\csc(a) + \cot(a)|}{|\csc(aS_\infty) + \cot(aS_\infty)|}} \quad (32)$$

For Step C., we find the inverse of f .

$$f(x) = \sin(ax) \implies f^{-1}(x) = \frac{\arcsin(x)}{a} \quad (33)$$

For Step D., substituting the expression for $\frac{1}{R_0}$ (32) and f^{-1} (33) into the overshoot equation (10) yields:

$$\text{Overshoot} = \frac{1}{a} \arcsin\left(\frac{a(S_\infty - 1)}{\ln\left(\frac{|\csc(a) + \cot(a)|}{|\csc(aS_\infty) + \cot(aS_\infty)|}\right)}\right) - S_\infty \quad (34)$$

For Step E., differentiation of both sides with respect to S_∞ and setting the equation to zero to solve for the critical S_∞^* yields:

$$0 = \frac{1}{a} \left(\frac{1}{\sqrt{1 - \left(\frac{a(S_\infty^* - 1)}{\ln\left(\frac{|\csc(a) + \cot(a)|}{|\csc(aS_\infty^*) + \cot(aS_\infty^*)|}\right)} \right)^2}} \right) \cdot \ln\left(\frac{|\csc(a) + \cot(a)|}{|\csc(aS_\infty^*) + \cot(aS_\infty^*)|}\right) \cdot a - a(S_\infty^* - 1) \cdot \frac{\frac{-|\csc(a) + \cot(a)| \cdot (-\cot(aS_\infty^*) \csc(aS_\infty^*) - a \csc^2(aS_\infty^*))}{(|\csc(aS_\infty^*) + \cot(aS_\infty^*)|)^2}}{\frac{|\csc(a) + \cot(a)|}{|\csc(aS_\infty^*) + \cot(aS_\infty^*)|}} - 1 \quad (35)$$

Solving this transcendental equation (35) requires first specifying the value of parameter a . For instance, specifying $a = 1$ and solving the equation numerically yields $S_\infty^* = 0.1648\dots$.

For Step F., we use S_∞^* in the overshoot equation (34) to obtain the value of the maximal overshoot for this model, $\text{Overshoot}^*|_{\beta(\sin(aS))I}$. For $a = 1$, we obtain:

$$\text{Overshoot}^*|_{\beta(\sin(S))I} = 0.2931\dots \quad (36)$$

Thus, the maximal overshoot for incidence functions of the form $\beta(\sin(S))I$ is 0.293... .

For Step G., we can calculate the corresponding R_0^* using S_∞^* and (32).

$$R_0^*|_{\beta(\sin(S))I} = 2.262\dots \quad (37)$$

Now consider $a = \frac{2\pi}{3}$, which produces a non-monotonic $f(S)$ over the unit interval (Figure S2a). Solving (35) for $a = \frac{2\pi}{3}$ yields $S_\infty^* = 0.1163\dots$. Repeating Steps F. and G. when $a = \frac{2\pi}{3}$ yields:

$$\text{Overshoot}^*|_{\beta(\sin(\frac{2\pi}{3}S))I} = 0.2529\dots \quad (38)$$

$$R_0^*|_{\beta(\sin(\frac{2\pi}{3}S))I} = 1.432\dots \quad (39)$$

This leads to the question of what the applicable domain of a is. The larger the value of a , the stronger the non-monotonicity of $f(S)$ is (Figure S2a). We can first eliminate values based on the second boundary condition (13) which requires that $f(S = 1) > \frac{1}{R_0}$. Clearly that condition is violated if $f(S = 1)$ is not positive, since $\frac{1}{R_0}$ is always positive because β and γ are both positive-definite. Since $f(S) = \sin(aS)$, then $f(S)$ is negative when $a \in [\pi n, 2\pi n]$, $n = \mathbb{N}$. Furthermore, since we have a formula for $\frac{1}{R_0}$ using (32), we can set up the inequality explicitly.

$$\begin{aligned} f(S = 1) &> \frac{1}{R_0} \\ \sin(a \cdot 1) &> \frac{a(S_\infty - 1)}{\ln\left(\frac{|\csc(a) + \cot(a)|}{|\csc(aS_\infty) + \cot(aS_\infty)|}\right)} \end{aligned}$$

These result for the different cases of $f(S) = \sin(aS)$ are shown in Figure S2b.

Time Series for Comparing Overshoot in Homogeneous and Heterogeneous Networks

To provide intuition on why heterogeneous networks can have higher overshoot at larger transmission compared to their more homogeneous counterparts, we look in the time-series data of the epidemic.

Shown is an example from a network with a very homogeneous network distribution ($\sigma = 0.000001$, Figure S4) and a moderately heterogeneous network ($\sigma = 0.000001$, Figure S5). The time series for a simulation on both networks is shown in Figure S3. Aside from σ , the other simulation parameters are held constant (i.e. number of nodes ($N=100$), transmission probability ($\tau = 0.1$), recovery probability ($\rho = 0.05$), number of initially infected individuals = 1, and mean degree = 7).

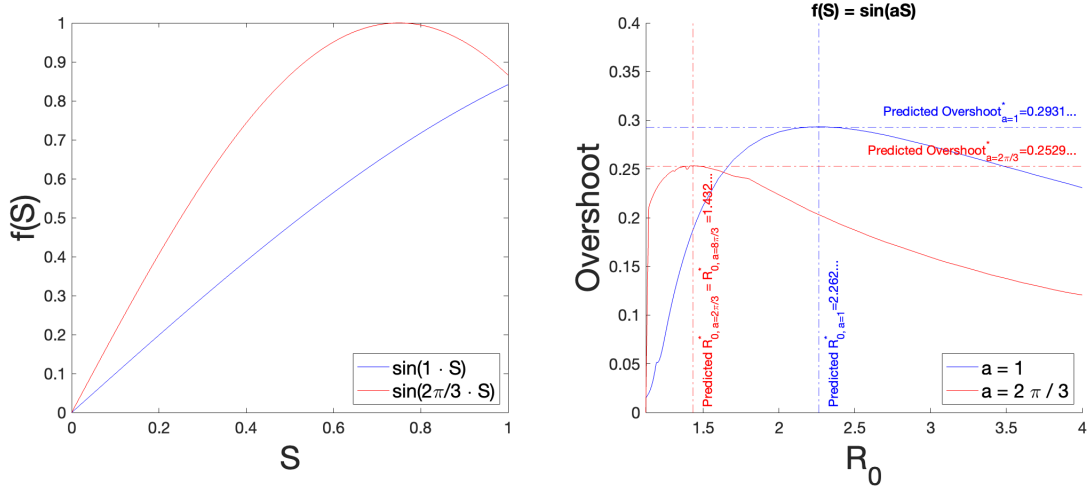


Figure S2: a) $f(S) = \sin(aS)$ for different values of a . b) The overshoot as a function of R_0 for an SIR model with nonlinear incidence term of $\beta(\sin(aS))I$ for different values of a . The dashed horizontal lines for $Overshoot^*$ and the dashed vertical lines for R_0^* are the theoretical predictions given by the calculations in the text. The solid curves are obtained from numerical simulations.

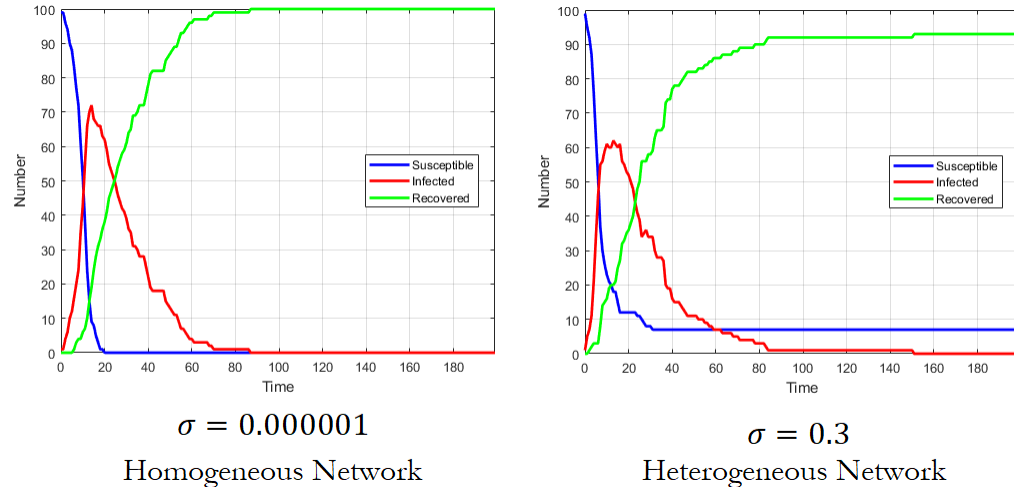


Figure S3: The time series for two network simulations that vary only in their heterogeneity parameter (σ). Left) The network is

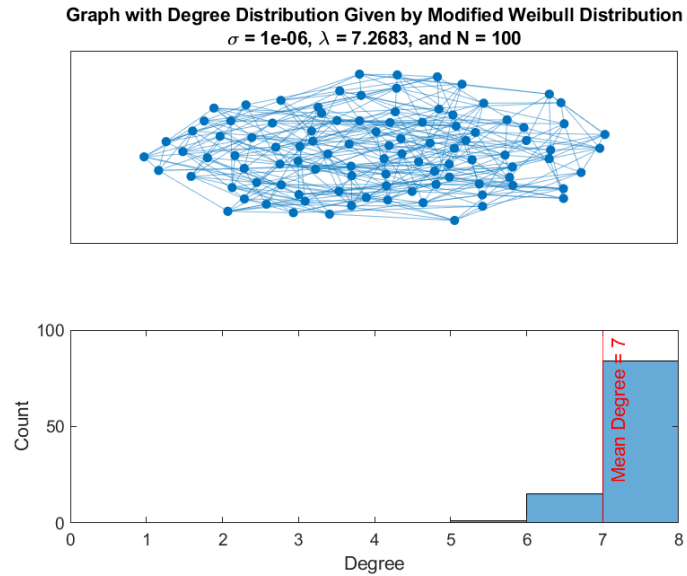


Figure S4: Network representation and corresponding degree distribution for a network with $\sigma = 0.000001$ (very homogeneous).

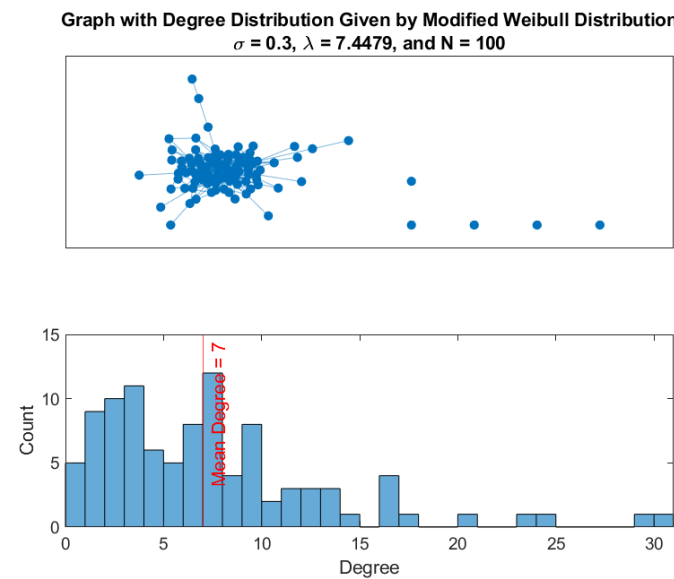


Figure S5: Network representation and corresponding degree distribution for a network with $\sigma = 0.3$ (moderate heterogeneity).

Supplemental Materials: Upper Bounds on Overshoot in the SIR Models with Nonlinear Incidence

Code to Generate Figures

Code executed in MATLAB R2023a.

```

42
43 %%%%%%
44 function [overshoot] = nonlinearIncidenceScript(numNodes, sigma,
45     weibullMean, transmissionProbability, recoveryProbability,
46     initialInfected, time)
47
48 close all
49
50 lambda = weibullMean ./ gamma(1+1./(-\text{log}(sigma))); %Scale parameter
51     . Sets middle of the probability distribution
52 adjacencyMatrix = generateModWeibullGraph(numNodes, sigma, lambda);
53
54 [epidemicDuration, finalAttackRate, overshoot] = simulateSIR(
55     adjacencyMatrix, transmissionProbability, recoveryProbability,
56     initialInfected, time, sigma, lambda);
57 end
58
59
60 %%%%%%
61 function [overshoot] = simulateSIR(adjacencyMatrix,
62     transmissionProbability, recoveryProbability, initialInfected, time,
63     sigma, lambda)
64 % Input:
65 % - adjacencyMatrix: The adjacency matrix representing the network.
66 % - transmissionProbability: Probability of transmission (infection)
67 %     between connected nodes per timestep..
68 % - recoveryProbability: Probability of recovery per timestep.
69 % - initialInfected: Number of initially infected individuals.
70 % - time: Total simulation timesteps.
71
72 % Number of nodes in the network
73 numNodes = size(adjacencyMatrix, 1);
74
75 % Initial state
76 susceptible = ones(numNodes, time);
77 infected = zeros(numNodes, time);
78 recovered = zeros(numNodes, time);
79
80 % Randomly select initially infected nodes
81 initialInfectedNodes = randperm(numNodes, initialInfected);
82 infected(initialInfectedNodes,1) = 1;
83 susceptible(initialInfectedNodes,1) = 0;
84 recovered(:,1) = zeros(numNodes, 1);
85
86 % Simulation loop
87 for timestep = 2:time
88
89     %% Calculate new infections probabilistically
90
91     potentialInfections = transmissionProbability * (adjacencyMatrix *
92         infected(:,timestep-1)) .* susceptible(:,timestep-1);
93     newInfections = double(rand(numNodes,1) < potentialInfections);
94
95     %% Calculate recoveries probabilistically
96     potentialRecoveries = recoveryProbability * infected(:,timestep-1); %
97         Recovery only occurs on previously infected nodes (not those
98         generated in current time step)
99     newRecovereds = double(rand(numNodes,1) < potentialRecoveries);

```

```

90 % Update states
91 susceptible(:,timestep) = susceptible(:,timestep-1) - newInfections;
92 infected(:,timestep) = infected(:,timestep-1) + newInfections -
93     newRecovereds;
94 recovered(:,timestep) = recovered(:,timestep-1) + newRecovereds;
95
96 if sum(infected(:,timestep)) == 0 && sum(infected(:,timestep-1)) > 0
97     epidemicDuration = timestep-1;
98 end
99
100 peakTime = find(sum(infected,1) == max(sum(infected,1)),1);
101 overshoot = (sum(susceptible(:,peakTime)) - sum(susceptible(:,end)))/
102     numNodes;
103 end
104
105
106 %%%%%%
107 function modWeibullGraph = generateModWeibullGraph(numNodes, sigma, lambda
108     )
109 % Input:
110 % - numNodes: Number of nodes in the graph.
111 % - sigma: The shape parameter for a 2-parameter modified Weibull
112 % distribution.
113 % - lambda: The median parameter for a 2-parameter modified Weibull
114 % distribution that centers the distribution.
115
116 %% Generate Degree Distribution based on modified 2-parameter Weibull
117 %% distribution (Ozbay and Nguyen)
118 alpha = -\text{log}(sigma);
119
120 distDraws = wblrnd(lambda, alpha, numNodes, 1);
121 degreeDistribution = round(distDraws);
122
123 %% Implement Configuration Model
124 adjacencyMatrix = zeros(numNodes);
125 numStubs = sum(degreeDistribution);
126 links = numStubs ./ 2;
127 stubs = zeros(numStubs, 1); %List of node IDs
128 dum = 0;
129 for i = 1:numNodes
130     stubs((dum+1):(dum+degreeDistribution(i))) = i;
131     dum = dum+degreeDistribution(i);
132 end
133
134 if mod(numStubs,2) == 0
135     link_counter = 0;
136     unique_nodes = numel(unique(stubs));
137
138     %Generate the network with neither self interactions nor multiple
139     %edges
140     while link_counter < links && unique_nodes > 1 && sum(sum(
141         adjacencyMatrix(unique(stubs), unique(stubs)))) < (unique_nodes^2 -
142         unique_nodes)
143         edge = randsample(numStubs, 2); %Sample 2 nodes from the stub list
144         %without replacement
145         if stubs(edge(1)) ~= stubs(edge(2)) && adjacencyMatrix(stubs(edge
146             (1)), stubs(edge(2))) == 0

```

```

138 adjacencyMatrix(stubs(edge(1)), stubs(edge(2))) = 1;
139 adjacencyMatrix(stubs(edge(2)), stubs(edge(1))) = 1;
140 link_counter = link_counter + 1;
141
142 %Delete the used stubs from the stub list and update the
143 %number of
144 %available stubs num_stubs. The entries of the stub list are
145 %put to NaN
146 %and then deleted to ensure the right stubs are deleted (
147 %deleting
148 %the 1st stub directly will shrink the list and make the
149 %second
150 %stub index invalid)!!! Also update the number of unique node
151 %IDs
152 %in the stub list
153 stubs(edge(1)) = NaN;
154 stubs(edge(2)) = NaN;
155 stubs(isnan(stubs)) = [];
156 numStubs = numel(stubs);
157 unique_nodes = numel(unique(stubs));
158
159 end
160
161
162
163
164
165
166
167
168
169
170
171
172
173
174
175
176
177
178
179
180
181
182
183
184
185
186

```

```
187 | end
188 |
189 modWeibullGraph = adjacencyMatrix;
190 end
```